and (3.11) of Ref. 2, when the pump-field amplitude in the latter relations is multiplied by the phase factor e^{ikz}.

[6]A general treatment of time-dependent linear susceptibilities for systems driven near resonance will be presented by the author in a subsequent publication.

[7]B. R. Mollow, Phys. Rev. **188**, 1969 (1969); Phys. Rev. A **2**, 76 (1970). The analysis of these papers is based on a quantum regression theorem derived by M. Lax [Phys. Rev. **172**, 350 (1968), and references cited therein].

[8]A realistic analysis of the frequency instability we have described would have to take into account the nonzero angular width of the pump wave.

PHYSICAL REVIEW A VOLUME 7, NUMBER 4 APRIL 1973

Low-Temperature Specific Heats of Adsorbed Helium Monolayers in the Mobile Limit*

Michael D. Miller and Chia-Wei Woo†
Department of Physics, Northwestern University, Evanston, Illinois 60201
(Received 2 October 1972)

Jackson's model for adsorbed helium monolayers is suitable for studying thermodynamic properties in the mobile limit. In particular, low-temperature specific heats can be calculated over a range of areal densities. The dominant contributions come from longitudinal surface phonons. We report here (i) an extension of Jackson's model to account for surface-phonon–surface-phonon interactions, (ii) computations of low-temperature specific heats to several coverages, and (iii) a comparison of the computed results to experiment.

I. ADSORBED HELIUM MONOLAYERS IN MOBILE LIMIT

Consider N helium atoms physically adsorbed on a smooth surface of a crystalline substrate. Let the adsorbing area be denoted by A. The system is then characterized by a single physical parameter: $n = N/A$, the areal density of the adsorbed layer.

Following our recent work published in Refs. 1 and 2, we make the preliminary approximation that the substrate serves no other purpose than to provide a static "external" field $V(\vec{r})$ to each adatom. The Hamiltonian of the system is then given by

$$H=\sum_{i=1}^{N}\frac{-\hbar^2}{2m}\nabla_i^2+\sum_{i=1}^{N}V(\vec{r}_i)+\sum_{1\le i<j\le N}v(r_{ij}), \tag{1}$$

where $\vec{r}$ is a three-dimensional vector and $v(r)$ represents the adatom-adatom interaction potential. In this work the pairwise, central Lennard-Jones 6-12 potential is used.

To solve the Schrödinger equation

$$H\psi(1, 2, \ldots, N)=E\psi(1, 2, \ldots, N) \tag{2}$$

for the ground state and the low-lying excited states, we proposed in Ref. 1 the employment of a set of correlated basis functions:

$$\phi_{\mu_1\vec{\nu}_1,\mu_2\vec{\nu}_2,\ldots,\mu_N\vec{\nu}_N}(z_1\vec{\rho}_1, z_2\vec{\rho}_2, \ldots, z_N\vec{\rho}_N) = F(1, 2, \ldots, N)P\left\{\prod_{i=1}^{N}\varphi_{\mu_i\vec{\nu}_i}(z_i\vec{\rho}_i)\right\}, \tag{3}$$

where F denotes a symmetrical correlating factor which accounts for the short-ranged adatom-adatom correlations and $\varphi_{\mu\nu}(z\vec{\rho})$ stands for the wave functions describing the motion of a single adatom, i.e., the eigenfunctions of the single-particle Hamiltonian:

$$h(\vec{r})=\frac{-\hbar^2}{2m}\nabla^2+V(\vec{r}). \tag{4}$$

The quantum number μ characterizes the bound states normal to the adsorbing surface (the z direction), and the two-component vector $\vec{\nu}$ characterizes motion parallel to that surface. For a realistic crystalline substrate, φ must clearly contain Bloch functions possessing the periodicity of the surface.

The subspace spanned by a set of basis functions of the type (3) with just one elementary excitation is of most importance when one considers low-temperature properties of the system. We take for this subspace $\mu_1=\mu$ and $\vec{\nu}_1=\vec{\nu}$, and $\mu_i=0$ and $\vec{\nu}_i=0$ for all $i\neq 1$. The basis functions of interest are then given by

$$\phi_{\mu\vec{\nu},00,\ldots,00}=\sum_{i=1}^{N}\left[\frac{\varphi_{\mu\vec{\nu}}(z_i\vec{\rho}_i)}{\varphi_{00}(z_i\vec{\rho}_i)}\right]\phi_0, \tag{5}$$

where

$$\phi_0\equiv\phi_{00,00,\ldots,00}=\prod_{i=1}^{N}\varphi_{00}(z_i\vec{\rho}_i), \tag{6}$$

and $\vec{\rho}$ is a two-component vector in a plane parallel to the adsorbing surface.

In the special case of a completely uniform and homogeneous substrate, the single-particle functions become

$$\varphi_{\mu\vec{\nu}}(z\vec{\rho})=\chi_\mu(z)e^{i\vec{\nu}\cdot\vec{\rho}}, \tag{7}$$

where $\vec{\nu}$ now represents a two-dimensional wave vector. Consequently Eq. (5) reduces to

$$\phi_{\mu\vec{\nu},00,\ldots,00}=\sum_{i=1}^{N}\left[\frac{\chi_\mu(z_i)e^{i\vec{\nu}\cdot\vec{\rho}_i}}{\chi_0(z_i)}\right]\phi_0, \tag{8}$$

giving rise to Jackson's model[3] of mobile adsorbed monolayers.

Jackson[3] classified the one-excitation states into two types: the longitudinal surface-phonon states,

$$\phi_{\vec{\nu}}^{L} \equiv \phi_{0\vec{\nu},00,\ldots,00} = \left[\sum_{i=1}^{N} e^{i\vec{\nu}\cdot\vec{\rho}_i}\right]\phi_0 = \rho_{\vec{\nu}}\phi_0 \,, \tag{9}$$

and the transverse surface-phonon states, which are essentially Eq. (8) with $\mu \neq 0$. Treating these surface phonons as elementary excitations obeying Bose statistics, he calculated their contribution to the low-temperature heat capacity and carried out numerical work for the transverse surface-phonons, assuming the substrate to consist of a layer of argon smeared out over a perfect metal with Cu parameters. He found the contribution to the heat capacity by the transverse surface phonons totally negligible at temperatures below 5 °K. For lack of information concerning ϕ_0, the contribution by the longitudinal surface phonons which actually dominate at low temperatures was not evaluated.

The purpose of this work is to (i) extend Jackson's model to include the effects of low-order surface-phonon–surface-phonon interactions, (ii) compute the heat capacity contributed by the longitudinal surface-phonons, and (iii) discuss the results in light of recent experimental findings by Dash,[4] Vilches,[5] and co-workers.

II. SURFACE-PHONON-SURFACE-PHONON INTERACTIONS

As in Feynman's theory of bulk helium,[6] an upper bound to the longitudinal surface-phonon spectrum can be determined variationally by evaluating the expectation value of H with respect to the trial wave function $\phi_{\vec{\nu}}^{L} = \rho_{\vec{\nu}}\phi_0$. Along with Jackson[3] we find, under the simplifying approximation

$$v(r_{ij}) \approx v(\rho_{ij}) \,, \tag{10}$$

that

$$\epsilon_\nu \leq \epsilon_\nu^0 = \frac{\langle \phi_{\vec{\nu}}^{L} | H | \phi_{\vec{\nu}}^{L} \rangle}{\langle \phi_{\vec{\nu}}^{L} | \phi_{\vec{\nu}}^{L} \rangle} - \frac{\langle \phi_0 | H | \phi_0 \rangle}{\langle \phi_0 | \phi_0 \rangle} = \frac{\hbar^2\nu^2}{2mS(\nu)} \,, \tag{11}$$

a result which is strictly valid only if ϕ_0 is the true ground-state wave function of the system. $S(\nu)$ is the two-dimensional liquid-structure function defined by

$$S(\nu) = 1 + n\int e^{i\vec{\nu}\cdot\vec{\rho}}[g(\rho) - 1]\,d\vec{\rho} \,, \tag{12}$$

with

$$g(\rho_{12}) = \frac{N(N-1)}{n^2}\,\frac{\int \phi_0^2\, d\vec{\rho}_3 \cdots d\vec{\rho}_N}{\int \phi_0^2\, d\vec{\rho}_1 \cdots d\vec{\rho}_N} \,. \tag{13}$$

The longitudinal surface-phonon heat capacity $C_L(T)$ is given by[3]

$$\frac{C_L(T)}{N} = \frac{1}{2\pi n k_B T^2}\int_0^\infty \frac{\epsilon_\nu^2\, e^{\epsilon_\nu/k_BT}\,\nu\,d\nu}{(e^{\epsilon_\nu/k_BT} - 1)^2} \,. \tag{14}$$

Preliminary numerical calculations to be presented in Sec. III indicate that ϵ_ν is linear at small ν and quadratic at large ν, as one would expect from sum rule arguments which apply in two dimensions as well as in three. For intermediate ν, say $0.3\ \text{Å}^{-1} \leq \nu \leq 3.0\ \text{Å}^{-1}$, the surface-phonon spectrum goes through an inflection, achieving a rotonlike dip if the areal density is sufficiently high. At very low temperatures, $C_L(T)$ is dominated by the linear portion of the spectrum. As the temperature exceeds 1 °K, the "roton" part begins to contribute significantly. An accurate determination of that part of the spectrum is therefore necessary. In bulk helium we learned that while the Feynman wave function is accurate in the long-wavelength limit, it is quantitatively worthless in the roton region: The roton gap obtained is more than twice the experimental value, giving rise to a heat capacity which is much too low. To remedy the situation, one must take into account phonon-phonon interactions, at least to the lowest order, either by modifying the trial wave function in the manner of Feynman and Cohen,[6] or by perturbative calculation in the manner suggested by Jackson and Feenberg.[7] Since the latter procedure is more transparent and can be systematically generalized by means of a canonical transformation,[8] we have chosen to adopt it for the present use.

Accordingly we go beyond the one-excitation subspace to include two-excitation basis functions:

$$\phi_{\mu\vec{\nu},\mu'\vec{\nu}',00,\ldots,00} = F(1,2,\ldots,N)P\{\varphi_{\mu\vec{\nu}}(z_1\vec{\rho}_1)\varphi_{\mu'\vec{\nu}'}(z_2\vec{\rho}_2)\varphi_{00}(z_3\vec{\rho}_3)\cdots\varphi_{00}(z_N\vec{\rho}_N)\}$$

$$= \sum_{1\leq i\neq j\leq N}\left[\frac{\varphi_{\mu\vec{\nu}}(z_i\vec{\rho}_i)\varphi_{\mu'\vec{\nu}'}(z_j\vec{\rho}_j)}{\varphi_{00}(z_i\vec{\rho}_i)\phi_{00}(z_j\vec{\rho}_j)}\right]\phi_0 = \sum_{i\neq j}\left[\frac{\chi_\mu(z_i)\chi_{\mu'}(z_j)e^{i\vec{\nu}\cdot\vec{\rho}_i + i\vec{\nu}'\cdot\vec{\rho}_j}}{\chi_0(z_i)\chi_0(z_j)}\right]\phi_0 \,. \tag{15}$$

Equation (15) includes longitudinal and transverse surface phonons as well as mixed surface phonon states. It will become clear presently that only pure longitudinal surface phonon states are important in this calculation. Thus we consider only the states

$$\phi_{0\vec{\nu},0\vec{\nu}',00,\ldots,00} = \sum_{i\neq j} e^{i\vec{\nu}\cdot\vec{\rho}_i + i\vec{\nu}'\cdot\vec{\rho}_j}\,\phi_0$$

$$= (\rho_{\vec{\nu}}\rho_{\vec{\nu}'} - \rho_{\vec{\nu}+\vec{\nu}'})\phi_0 \,. \tag{16}$$

And since the set $\phi_{\vec{\nu}}^{L}$ of Eq. (9) includes the second term of Eq. (16), it is sufficient and indeed more

convenient to consider

$$\phi^L_{\vec{\nu},\vec{\nu}'} \equiv \rho_{\vec{\nu}}\rho_{\vec{\nu}'}\phi_0 , \tag{17}$$

which hereafter will be referred to as two-surface-phonon functions. We find

$$\frac{\langle \phi^L_{\vec{\nu},\vec{\nu}'} | H | \phi^L_{\vec{\nu},\vec{\nu}'} \rangle}{\langle \phi^L_{\vec{\nu},\vec{\nu}'} | \phi^L_{\vec{\nu},\vec{\nu}'} \rangle} = \frac{\langle \phi_0 | H | \phi_0 \rangle}{\langle \phi_0 | \phi_0 \rangle} + \epsilon^0_\nu + \epsilon^0_{\nu'} , \tag{18}$$

and the three-surface-phonon matrix element

$$\langle \vec{\nu} | H | \vec{\nu} - \vec{\nu}', \vec{\nu}' \rangle \equiv (\langle \phi^L_{\vec{\nu}} | H | \phi^L_{\vec{\nu}-\vec{\nu}',\vec{\nu}'} \rangle - \epsilon^0_\nu \langle \phi^L_{\vec{\nu}} | \phi^L_{\vec{\nu}-\vec{\nu}',\vec{\nu}'} \rangle)/(\langle \phi^L_{\vec{\nu}} | \phi^L_{\vec{\nu}} \rangle \langle \phi^L_{\vec{\nu}-\vec{\nu}',\vec{\nu}'} | \phi^L_{\vec{\nu}-\vec{\nu}',\nu'} \rangle)^{1/2}$$

$$\simeq \frac{\hbar^2}{2m}[NS(\nu)S(|\vec{\nu}-\vec{\nu}'|)S(\nu')]^{-1/2}\{\nu^2 S(\nu')[1 - S(|\vec{\nu}-\vec{\nu}'|)] + \vec{\nu}\cdot\vec{\nu}'[S(|\vec{\nu}-\vec{\nu}'|) - S(\nu')]\} . \tag{19}$$

The latter required the use of Kirkwood's superposition approximation for the three-particle distribution function:

$$g_3(\rho_{12}, \rho_{23}, \rho_{31}) \equiv \frac{N(N-1)(N-2)}{n^3} \frac{\int \phi_0^2 d\vec{\rho}_4 \cdots d\vec{\rho}_N}{\int \phi_0^2 d\vec{\rho}_1 \cdots d\vec{\rho}_N}$$

$$\simeq g(\rho_{12})\, g(\rho_{23})\, g(\rho_{31}) . \tag{20}$$

The leading correction to Feynman's spectrum ϵ^0_ν can be obtained by second-order Brillouin-Wigner perturbation theory[7] using the three-surface-phonon matrix element as the perturbation. An implicit equation for the perturbed energy spectrum ϵ_ν is obtained:

$$\epsilon_\nu = \epsilon^0_\nu + \frac{1}{2}\sum_{\vec{\nu}'\neq 0} \frac{|\langle \vec{\nu} | H | \vec{\nu}-\vec{\nu}', \vec{\nu}' \rangle|^2}{\epsilon_\nu - \epsilon^0_{|\vec{\nu}-\vec{\nu}'|} - \epsilon^0_{\nu'}} . \tag{21}$$

Measuring energy in units of $\hbar^2/2m$ Å^{-2},

$$E_\nu \equiv \epsilon_\nu/(\hbar^2/2m\ \text{Å}^{-2}) ,$$
$$E^0_\nu \equiv \epsilon^0_\nu/(\hbar^2/2m\ \text{Å}^{-2}) = \nu^2/S(\nu)\ ^\circ\text{K Å}^2 , \tag{22}$$

and writing

$$\nu'' \equiv |\vec{\nu}-\vec{\nu}'| = (\nu^2 + \nu'^2 - 2\nu\nu'\cos\theta)^{1/2} , \tag{23}$$

we find

$$E_\nu = E^0_\nu + \frac{1}{4\pi^2 n}\int_0^\infty d\nu' \int_0^\pi d\theta \times \frac{\nu'\{\nu^2 S(\nu')[1 - S(\nu'')] + \nu\nu'\cos\theta[S(\nu'') - S(\nu')]\}^2}{S(\nu)S(\nu')S(\nu'')[E_\nu - E^0_{\nu'} - E^0_{\nu''}]} , \tag{24}$$

an equation which can be solved by iteration or by graphs.

Note that in principle the intermediate states in Eq. (21) should not be limited to two longitudinal surface phonons. However, practicality (as well as experience with bulk helium) dictates that matrix elements involving more than two surface phonons can be disregarded. Also, intermediate states containing transverse surface phonons do not contribute significantly since on the one hand the energy denominator will increase by a sizable amount, and on the other hand the matrix element in the numerator will decrease as a result of nodes appearing in the single-particle functions.

III. CALCULATIONS AND RESULTS

The discussion in the last section suggests that the only quantity required for evaluating $C_L(T)$ is the liquid structure function $S(\nu)$. The definition of $S(\nu)$ through Eqs. (12) and (13) is identical to that defining the liquid-structure function of a two-dimensional system.

In a recent paper,[9] we reported on detailed calculations for the ground state of two-dimensional helium. Variational wave functions of the Jastrow form

$$\phi_0(1, 2, \ldots, N) = \prod_{i<j} e^{u(\rho_{ij})/2} \tag{25}$$

were employed, in terms of which two- and three-particle distribution functions were defined, as in Eqs. (13) and (20). Parametric forms of $u(\rho)$ were chosen and the energy expectation value $E_0 = \langle \phi_0 | H | \phi_0 \rangle / \langle \phi_0 | \phi_0 \rangle$ was minimized with respect to $u(\rho)$. The crucial task in such a calculation is the determination of $g(\rho)$ for every given choice of $u(\rho)$; this was accomplished by means of several well-known integral-equation techniques, which confirmed and improved earlier results of computer experiments. Further confidence was gained when these results were checked out by the use of a highly efficient Monte Carlo program which was developed for another purpose.[10]

From Ref. 9 we borrow the radial distribution function $g(\rho)$ and the ground-state energy E_0 for a range of areal densities, n. The knowledge of $g(\rho)$ gives us $S(\nu)$ which, however, is accurate only in the regions of intermediate and large ν. This is because the small-ν behavior of $S(\nu)$ depends on the long-range behavior of $g(\rho)$, and the latter cannot be accurately determined by variational calculations such as that of Ref. 9, even with the inclusion of proper long-range parts in $u(\rho)$ according to the procedure proposed by Chester and Reatto.[11] There is however an alternate way of determining $S(\nu)$ at long wavelengths. As in bulk helium,

$$S(\nu) \to \hbar\nu/2mc \quad \text{as} \quad \nu \to 0 , \tag{26}$$

where c denotes the velocity of sound, a quantity that can be obtained from the energy-density rela-

tion (the equation of state):

$$c = 1/(mn\kappa)^{1/2}, \tag{27}$$

where

$$\kappa = \left(2n^2 \frac{d(E_0/N)}{dn} + n^3 \frac{d^2(E_0/N)}{dn^2}\right)^{-1}. \tag{28}$$

An interpolation between the small and intermediate ν regions then completes $S(\nu)$. The error caused by this rather arbitrary interpolation procedure is imperceptible as far as specific heats are concerned.[12]

Figure 1 shows the energy-density relation used. $g(\rho)$ is available at four areal densities: 0.030, 0.036, 0.046, and 0.056 Å^{-2}; $n = 0.036$ Å^{-2} corresponds to zero surface tension and is shown in Fig. 2. The corresponding $S(\nu)$ and ϵ_ν^0 are given in Figs. 3 and 4, respectively. At this low areal density the roton region degenerates to a mere inflection. A more recognizable roton can be identified at $n = 0.056$ Å^{-2}; it is also shown in Fig. 4 for comparison.

The renormalization of surface phonons by means of the second-order Brillouin-Wigner calculation outlined in Sec. II gives rise to energy corrections which are too small to be of significance. Even for $n = 0.056$ Å^{-2} the lowering of the roton dip is merely a few percent. We conclude that it is sufficiently reliable to use ϵ_ν^0 in place of ϵ_ν. The fact that the corrections are small is no doubt connected to the low densities with which we are concerned. The bulk helium density of 0.0218 Å^{-3} scales to $n = 0.075$ Å^{-2}, which is much higher than the range of areal densities considered here.

The low-temperature heat capacities computed for $n = 0.036$, 0.046, and 0.056 Å^{-2} are presented in Figs. 5, 6, and 7, respectively. In the case of $n = 0.030$ Å^{-2}, the areal density is below the zero-tension value and one must consider two-phase equilibrium.

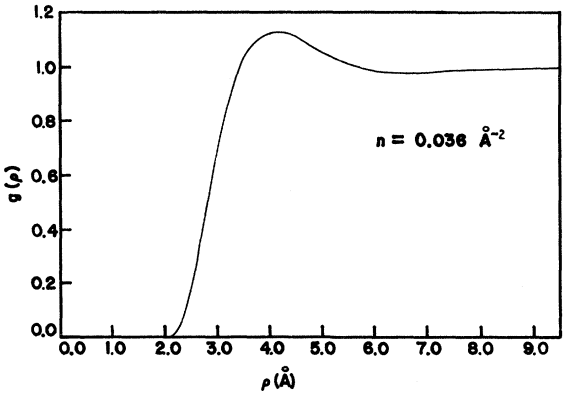

FIG. 2. Two-particle radial distribution function for two-dimensional He^4 shown at the equilibrium density.

IV. DISCUSSION

For areal densities above 0.036 Å^{-2}, the helium monolayer will be under tension, but will remain a monolayer. The cost in energy is too high for forming a second layer, as demonstrated by a crude calculation discussed in the Appendix. We therefore have on hand three sets of specific-heat calculations to compare with experiment.

Stewart and Dash[4] carried out extensive heat-capacity measurements for He^4 adsorbed on argon-plated copper sponge. Their best estimate of the adsorbing area is 46.75 m^2, and a full monolayer coverage requires 13.2 cm^3 of He^4. This corresponds to an areal density of 0.076 Å^{-2}. In Figs. 5 and 7 we include their data for $x = 0.5$ ($n = 0.038$ Å^{-2}), and $x = 0.7$ ($n = 0.053$ Å^{-2}). Our results are in qualitative agreement with these data. Dash, however, contends[13] that their high-temperature data

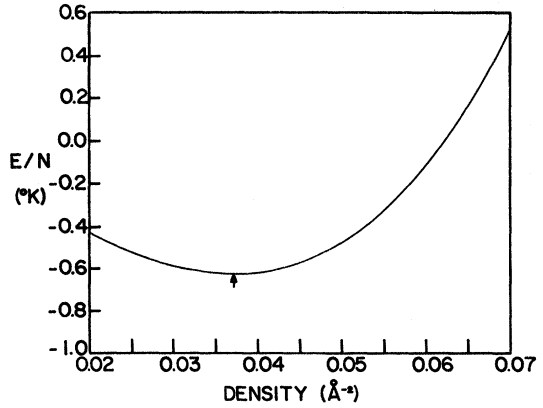

FIG. 1. Total energy per particle for the two-dimensional He^4 system obtained by a variational calculation as described in Ref. 9. The arrow locates the energy minimum.

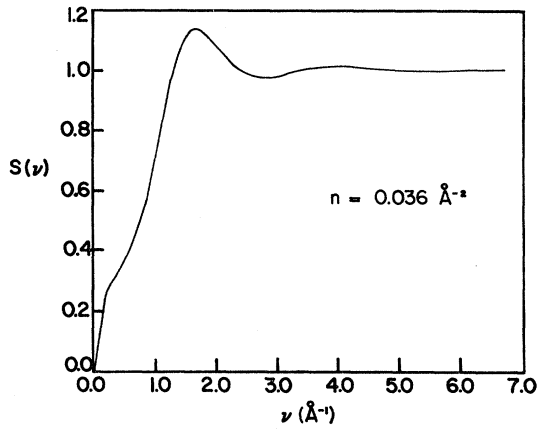

FIG. 3. Liquid-structure function calculated from the radial distribution function shown in Fig. 2.

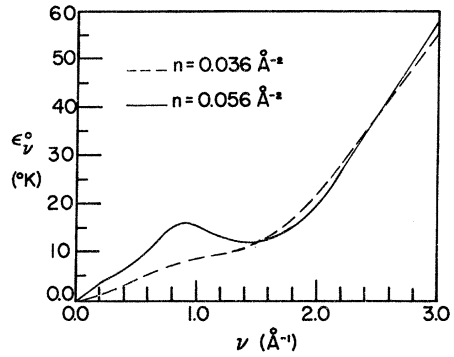

FIG. 4. Energy spectra at $n=0.036$ Å^{-2} and $n=0.056$ Å^{-2} showing the onset of a rotonlike dip as the density is increased.

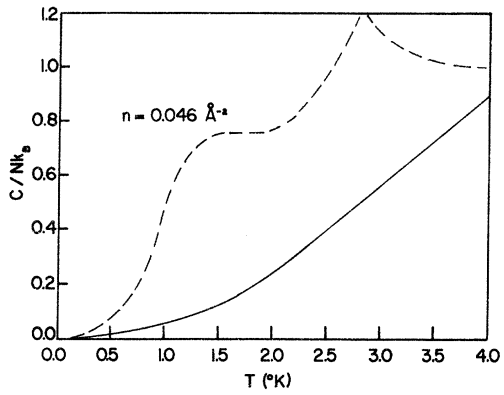

FIG. 6. The specific heat at $n=0.046$ Å^{-2}: solid line, calculated; dashed line, eyeball fit to the data of McLean (Ref. 5).

for low coverages do not approach the proper two-dimensional asymptotic value of Nk_B. Consequently the substrate surface could not have been free of inhomogeneities, and our own simple model cannot apply here.

Hickernell, McLean, and Vilches[5] performed similar measurements on exfoliated graphite, and found that at high temperatures the data indeed approach Nk_B. It is suggested[13] that the substrate surface is smoother and perhaps our model would be more realistic for this set of experiments—at least at temperatures low compared to the transition temperatures discussed in Ref. 5. These data are shown in Figs. 5 and 7 (full coverage corresponds to $n=0.1$ Å^{-2}). We find no agreement at all. The reason is probably as follows. As pointed out by Hickernell *et al.*,[5] the periodic structure of the substrate may still be an important factor. Also, in our model, the substrate has not been permitted to play a dynamic role. It serves no other purpose than to restrict the adatoms to near-planar motion. In reality, the substrate excitations help to mediate adatom-adatom interactions. In place of the bare He-He interaction $v(r)$, a somewhat more attractive effective potential should appear in the Hamiltonian of Eq. (1).[14] A microscopic calculation[15] of the latter is at present under way. The calculation reported in this paper will be repeated when such an effective potential becomes available.

APPENDIX

Within the framework of Jackson's model of He^4 monolayers it is simple to make a crude estimate of how much energy it would take to lift a particle out of the monolayer to begin formation of a "second layer." In Jackson's model the Hamiltonian, Eq. (1), is separable into two additive parts: one concerned with motion parallel to the substrate and the other with motion normal to it. Thus, the energy eigenvalue is also separable and can be written

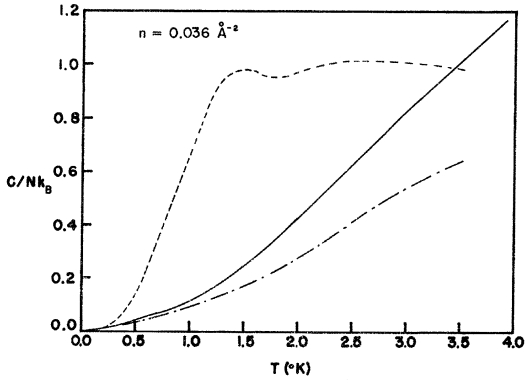

FIG. 5. Specific heat at $n=0.036$ Å^{-2}: solid line, calculated ; dashed line, eyeball fit to the data of McLean (Ref. 5); dot-dashed line, eyeball fit to the data of Stewart and Dash (Ref. 4).

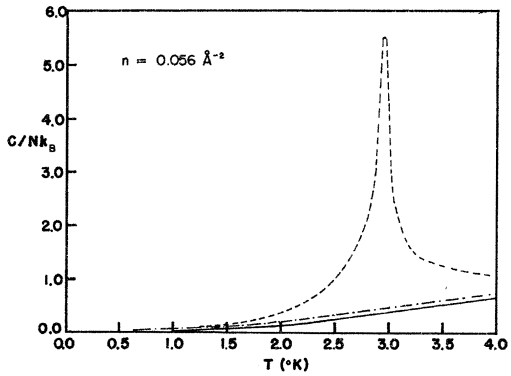

FIG. 7. The specific heat at $n=0.056$ Å^{-2}: solid line, calculated; dashed line, eyeball fit to the data of McLean (Ref. 5); dot-dashed line, eyeball fit to the data of Stewart and Dash (Ref. 4).

$$\epsilon_1 = \epsilon_\perp + \epsilon_\parallel \ . \tag{A1}$$

The parallel contribution can be immediately read off Fig. 1 and at the highest density used in this paper, $n = 0.056$ Å^{-2},

$$\epsilon_\parallel = -0.29\ ^\circ\mathrm{K} \ . \tag{A2}$$

The normal contribution $\epsilon_\perp$ is just the ground-state eigenvalue of the Hamiltonian, Eq. (4),

$$\left[-\frac{\hbar^2}{2m}\frac{d^2}{dz^2} + \left(\frac{\alpha_s}{z^9} - \frac{\beta_s}{z^3}\right)\right]\chi_0(z) = \epsilon_1\chi_0(z) , \tag{A3}$$

where

$$\alpha_s \equiv \tfrac{1}{45}\pi d\epsilon r_m^{12} \ , \quad \beta_s \equiv \tfrac{1}{6}\pi d 2\epsilon r_m^6 \ . \tag{A4}$$

ϵ and r_m are the Ar-He Lennard–Jones-potential parameters taken from molecular-beam experiments[1]:

$$\epsilon = 25.4\ ^\circ\mathrm{K} \ , \quad r_m = 3.4\ \text{Å} \ . \tag{A5}$$

d is the argon substrate number density assuming an Ar liquid with the same density as the fcc solid:

$$d = 0.0251\ \text{Å}^{-3} \ . \tag{A6}$$

Equation (A3) was solved numerically using the Numerov technique familiar to atomic-structure calculations.[16] The ground-state energy obtained is

$$\epsilon_\perp = -21.29\ ^\circ\mathrm{K} \ . \tag{A7}$$

Thus the total energy per particle for a He^4 atom in the first monolayer at a density of 0.056 Å^{-2} is

$$\epsilon_1 = -21.58\ ^\circ\mathrm{K} \ . \tag{A8}$$

To complete the calculation we need the ground state energy of a single He^4 atom placed over a flat, uniform He^4 monolayer which lies a distance z_0 above a uniform Ar substrate. z_0 is chosen as the expectation value of z calculated with the ground-state eigenfunction χ_0 of Eq. (A3). The Hamiltonian for such a system can be written as

$$h(z) = -\frac{\hbar^2}{2m}\frac{d^2}{dz^2} + \left(\frac{\alpha_m}{(z-z_0)^{10}} - \frac{\beta_m}{(z-z_0)^4}\right) + \left(\frac{\alpha_s}{z^9} - \frac{\beta_s}{z^3}\right) \ , \tag{A9}$$

where

$$\alpha_m = \tfrac{1}{5}\pi n 4\epsilon\sigma^{12} \ , \quad \beta_m = \tfrac{1}{2}\pi n 4\epsilon\sigma^6 \ . \tag{A10}$$

The substrate potential parameters α_s and β_s were previously defined in Eq. (A4). In Eq. (A10), n is the monolayer number density as usual and ϵ and σ are the He-He Lennard–Jones-potential parameters

$$\epsilon = 10.22\ ^\circ\mathrm{K} \ , \quad \sigma = 2.556\ \text{Å} \ . \tag{A11}$$

The eigenvalue solution of Eq. (A9) is again done numerically by the Numerov technique, which yields for the ground-state energy

$$\epsilon_2 = -7.03\ ^\circ\mathrm{K} \ . \tag{A12}$$

The difference in energy, $\Delta\epsilon$, between a He^4 atom in the monolayer and one in the first available single-particle state above the monolayer (the "second layer") is thus

$$\Delta\epsilon = 14.5\ ^\circ\mathrm{K} \ . \tag{A13}$$

The energy $\Delta\epsilon$ is considerably larger than the temperatures characteristic of this problem. We interpret this to indicate that at the densities investigated in this paper "second layer" formation due to boiling particles out of the first layer is not an important process.

This calculation could be extended to a more realistic system but the result would be, in general, to increase the energy difference $\Delta\epsilon$. For example, instead of the totally smeared out potential of Eq. (A3), a fit to the lattice summed potential (like V_0 in Ref. 1) could be used. The well of V_0 is 50% deeper than the smeared out potential and yields a ground-state eigenvalue of about $-45\ ^\circ$K. In this model, ϵ_2 [Eq. (A12)] is rather insensitive to the substrate potential since the monolayer acts to shield the single-particle states above it from the substrate below it. Thus $\Delta\epsilon$ will now be in the neighborhood of 35 °K.

The equation of state shown in Fig. 1 and calculated in Ref. 9 (using the BBGKY integral equation) is too soft at higher densities; thus, by employing a stiffer equation of state one could increase $\epsilon_\parallel$ in a direction which would favor second-layer formation. A Monte Carlo equation of state[10] yields an energy of $+0.2\ ^\circ$K at $n = 0.056$ Å^{-2}. The difference of 0.5 °K between the two equations of state is certainly not sufficient to bring $\Delta\epsilon$ into the low-temperature range at which the monolayer systems are explored.

---

*Work supported in part by the National Science Foundation through Grant No. GP-29130 and by the Advanced Research Projects Agency through the Materials Research Center of Northwestern University.

†Alfred P. Sloan Research Fellow.

[1]H.-W. Lai, C.-W. Woo, and F. Y. Wu, J. Low Temp. Phys. **3**, 463 (1970).

[2]H.-W. Lai, C.-W Woo, and F. Y. Wu, J. Low Temp. Phys. **5**, 499 (1971).

[3]H. W. Jackson, Phys. Rev. 180, 184 (1969).

[4]G. A. Stewart and J. G. Dash, Phys. Rev. A **2**, 918 (1970); and the references quoted therein.

[5]D. C. Hickernell, E. O. McLean, and O. E. Vilches, Phys. Rev. Lett. **28**, 789 (1972); and E. O. McLean, Ph. D. thesis, (University of Washington, 1972) (unpublished), and the references quoted therein.

[6]See for example J. Wilks, *The Properties of Liquid and Solid Helium* (Clarendon, Oxford, England, 1967).

[7]H. W. Jackson and E. Feenberg, Rev. Mod. Phys. **34**, 686 (1962).

[8]C.-W. Woo, H. T. Tan, and W. E. Massey, Phys. Rev. **185**, 287 (1969).

[9]C. E. Campbell and M. Schick, Phys. Rev. A **3**, 691 (1971); and M. D. Miller, C.-W. Woo, and C. E. Campbell, Phys. Rev. A **6**, 1942 (1972).

[10]R. L. Coldwell and C.-W. Woo (unpublished).

[11]In a calculation to be reported elsewhere, one of us (M. D. M.) has been unable to reproduce the bulk-helium results reported by W. P. Francis, G. V. Chester, and L. Reatto [Phys. Rev. A **1**, 86 (1970)]. The BBGKY integral equation was employed rather than the PY2XS used by Francis, Chester, and Reatto.

[12]Even if the small-ν (< 0.2 Å^{-1}) corrections to $S(\nu)$ were omitted altogether the effect on the specific heat would be negligible except at the lowest temperatures (<0.5 °K). By introducing the linear extrapolation, one depresses the value of the specific-heat integrand, Eq. (14), at small ν and consequently reduces the specific heat. As the temperature is raised, the intermediate region of the spectrum makes increasingly appreciable contributions to the specific-heat integrand and quickly tends to dominate the effect of the linear region. At $n = 0.036$ Å^{-2}, for example, the heat capacity per unit area (cf., Fig. 5) at $T = 0.1$ °K is 0.11×10^{-3} Å^{-2}; without the linear extrapolation it is 0.24×10^{-3} Å^{-2}. At $T = 0.5$ °K, the heat capacity with the linear extrapolation is 0.152×10^{-2} Å^{-2} and without it is 0.155×10^{-2} Å^{-2}. For $T > 1$ °K the differences are imperceptible. Thus, we can expect that the specific heat will be rather insensitive to a detail such as the proper connection between the small-ν and intermediate-ν regions of $S(\nu)$.

[13]J. G. Dash (private communication).

[14]M. Schick and C. E. Campbell, Phys. Rev. A **2**, 1591 (1970).

[15]C.-W. Woo, J. Low Temp. Phys. **3**, 335 (1970).

[16]See, for example, D. R. Hartree, *The Calculation of Atomic Structures* (Wiley, New York, 1957), p. 71; and F. Herman and S. Skillman, *Atomic Structure Calculations* (Prentice-Hall, Englewood Cliffs, N. J., 1963).

PHYSICAL REVIEW A VOLUME 7, NUMBER 4 APRIL 1973

Pressure Dependence of Self-Generated Magnetic Fields in Laser-Produced Plasmas*

R. S. Bird, L. L. McKee,† F. Schwirzke, and A. W. Cooper
Naval Postgraduate School, Monterey, California 93940
(Received 5 September 1972)

The systematic dependence of the magnitude of the self-generated magnetic fields of a laser-produced plasma on nitrogen background pressure has been investigated. At expansion distances of a few millimeters or more, the strongest fields were found to reside at the front of the streaming laser plasma. Magnetic fields were created in the laser plasma long after laser shut off by allowing the streaming plasma to impinge upon a glass plate.

Magnetic fields spontaneously generated in the absence of applied fields have been observed in several experiments with laser-produced plasmas.[1-3] Stamper *et al.*[3] have suggested that these spontaneous fields result from thermo-electric currents associated with temperature and pressure gradients existing during the early stages of the formation and heating of a plasma by a giant laser pulse.

We have made a systematic study of the dependence of the spontaneous magnetic fields on the pressure of the background gas which indicates that magnetic fields are generated by pressure gradients in the front of the expanding laser plasma. Field amplification or field reversal can be caused by increase or reversal of the pressure gradients in the plasma front long after the end of the laser pulse.

The equation describing the development of the magnetic fields is obtained from the generalized Ohm's law

$$\vec{J} = \sigma [\vec{E} + \vec{V}_e \times \vec{B} + (1/en_e) \nabla P_e] , \qquad (1)$$

where all quantities have their conventional meaning and the subscript e refers to the electron component of that quantity. Solving for $\vec{E}$ and using

$$\nabla \times \vec{E} = -\frac{\partial \vec{B}}{\partial t}$$

gives

$$\frac{\partial \vec{B}}{\partial t} = \nabla \times (\vec{V}_e \times \vec{B}) + \frac{1}{\mu_0 \sigma} \nabla^2 \vec{B} + \frac{k}{en_e} \nabla T_e \times \nabla n_e . \qquad (2)$$

The first two terms on the right-hand side are the flow and diffusion terms. The generation of a magnetic field requires that the last term, the source term $\vec{S}$, be nonzero.

The beam from a 300-MW (7.5 J in 25 nsec) neodymium-doped glass laser was focused by a lens with a 28-cm focal length. The principal targets were aluminum and Mylar discs. The laser irradiation produced a 2-mm hole in the Mylar (disc thickness 0.01 cm) but did not penetrate the aluminum. The laser beam entered a vacuum chamber and struck the target at an angle of 30° with respect to the target normal. The resultant plasma streamed out along the target normal[4] defining a convenient cylindrical-polar coordinate system with the z axis along the target normal, the $\theta = 0°$ line vertically up, and the origin centered on the burn spot. The magnetic field was analyzed with small